Structure and the location of the morphotropic phase boundary region in (1-x)[Pb($Mg_{1/3}Nb_{2/3}$)O_3]-xPbTiO_3

2001 J. Phys.: Condens. Matter 13 L931

(http://iopscience.iop.org/0953-8984/13/48/102)

INSTITUTE OF PHYSICS PUBLISHING JOURNAL OF PHYSICS: CONDENSED MATTER

J. Phys.: Condens. Matter **13** (2001) L931–L936 PII: S0953-8984(01)29801-4

LETTER TO THE EDITOR

Structure and the location of the morphotropic phase boundary region in $(1 - x)[Pb(Mg_{1/3}Nb_{2/3})O_3]$–$xPbTiO_3$

Akhilesh Kumar Singh and Dhananjai Pandey

School of Materials Science and Technology, Institute of Technology, Banaras Hindu University, Varanasi 221005, India

E-mail: dpandey@banaras.ernet.in

Received 17 October 2001
Published 16 November 2001
Online at stacks.iop.org/JPhysCM/13/L931

Abstract

The structure of $(1 - x)[Pb(Mg_{1/3}Nb_{2/3})O_3]$–$xPbTiO_3$ is tetragonal and rhombohedral for $x \geqslant 0.35$ and $x \leqslant 0.30$, respectively. The intrinsic width of the morphotropic phase boundary region ($0.30 < x < 0.35$) is an order of magnitude smaller than hitherto believed. The structure of the morphotropic phase for $x = 0.34$ is shown to be monoclinic with space group Pm and not a mixture of rhombohedral and tetragonal phases.

The phase diagram of solid solutions of $PbTiO_3$ with materials such as $PbZrO_3$, $Pb(Mg_{1/3}Nb_{2/3})O_3$, and $Pb(Zn_{1/3}Nb_{2/3})O_3$ exhibits a nearly vertical morphotropic phase boundary (MPB) separating tetragonal and rhombohedral phase fields [1–3]. Currently there is a lot of interest in the physics of materials showing MPB characteristics. Of these, the $Pb(Zr_xTi_{1-x})O_3$ (PZT) system has attracted enormous interest in recent years [4–12]. Noheda *et al* [5] have discovered a tetragonal-to-monoclinic phase transition below room temperature for $x = 0.50$ and 0.52 using high-resolution x-ray powder diffraction data. Ragini *et al* [9] subsequently discovered that this monoclinic phase undergoes an antiferrodistortive phase transition into another monoclinic phase with doubled lattice constant in the [001] direction [11]. The characteristic superlattice reflections for the second monoclinic phase are present in the selected-area electron diffraction [9] and neutron diffraction [11] patterns but not in the x-ray diffraction pattern, as a result of which Noheda *et al* [5] missed it. Noheda *et al* [6] have proposed that the structure of PZT in the MPB region, separating the tetragonal and rhombohedral phase fields at the Ti- and Zr-rich ends, respectively, is monoclinic at 300 K. Ragini *et al* [12] have carried out a Rietveld analysis of the room temperature (300 K) x-ray powder diffraction data for PZT and shown that the structure is tetragonal (space group $P4mm$) for $x \leqslant 0.515$ whereas for $x = 0.520$ and 0.525, the tetragonal and monoclinic (space group Cm) phases coexist. From a careful analysis of the anomalous broadening of the

$h00$- and $hh0$-type reflections, Ragini *et al* [12] have further shown that the structure of PZT for $0.53 \leqslant x \leqslant 0.62$ (i.e., on the Zr-rich side of the MPB) is not rhombohedral, as hitherto believed, but monoclinic.

The recent discoveries in relation to PZT have been followed up in other MPB systems such as $(1-x)$[Pb($Mg_{1/3}Nb_{2/3}$)O_3]–xPbTiO_3 (PMN–xPT) and $(1-x)$[Pb($Zn_{1/3}Nb_{2/3}$)O_3]–xPbTiO_3 (PZN–xPT). On the basis of a high-resolution synchrotron x-ray diffraction study of a poled single crystal of PMN–0.35PT, Ye *et al* [13] have recently proposed that the structure of the morphotropic phase in this system is monoclinic with space group Cm, similar to that in PZT. In the related PZN–xPT system, Yesu *et al* [14] have proposed that the structure of the morphotropic phase could be either monoclinic with space group Pm or orthorhombic with space group $Bmm2$. In the present work, we have carried out a detailed Rietveld analysis of the x-ray powder diffraction data for the morphotropic phase composition in the PMN–xPT system with $x = 0.34$. It is shown that the most likely space group of the morphotropic phase in the PMN–xPT system is Pm and not Cm. We have also attempted to locate the MPB region very precisely.

PMN–xPT samples normally contain a small amount of an unwanted pyrochlore phase unless excess amounts of MgO and PbO are used [15]. We have developed a new method [16] for the preparation of pyrochlore-free PMN–xPT samples of excellent quality without using excess amounts of MgO and PbO. In this method, the columbite precursor $MgNb_2O_6$ was prepared by calcining a stoichiometric mixture of $MgCO_3{\cdot}3H_2O$ (99%), instead of MgO as used by earlier workers [15], and Nb_2O_5 (99.95%) at 1050 °C for 6 h. At the next stage, the stoichiometric amount of TiO_2 was added to $MgNb_2O_6$ and calcined at 1050 °C for another 6 h to obtain $(1-x)/3MgNb_2O_6$–$(x)TiO_2$ (MNT) precursor. This MNT precursor was then mixed with the stoichiometric amount of $PbCO_3$ (99%), instead of PbO as used by earlier workers [15], and calcined at 750 °C for 6 h to obtain pure perovskite phase powders of PMN–xPT free from pyrochlore phase. Sintering was carried out at 1150 °C for 6 h in sealed crucibles with a PbO atmosphere to get samples with densities greater than 99% of the theoretical value. The sintered pellets were crushed into fine powders and then annealed at 500 °C for 10 h to remove the strains introduced during crushing. XRD data were collected using a 12 kW rotating-anode- (Cu-) based Rigaku powder diffractometer operating in the Bragg–Brentano geometry and fitted with a graphite monochromator in the diffracted beam. The XRD data were recorded at $\Delta(2\theta) = 0.02^\circ$ intervals in the 2θ range 20°–120° at a scan speed of 1° min^{-1}.

In order to locate the MPB region in the sintered powders, we have analysed the pseudocubic 200, 220, and 222 reflections of different PMN–xPT compositions shown in figure 1. For the tetragonal phase, the 200 pseudocubic reflection is a doublet while 222 is a singlet. Further, 220 is also a doublet with the stronger peak corresponding to the 202 reflection occurring at the lower-2θ side of the weaker 220 reflection. The structure of PMN–xPT is found to be tetragonal for $x \geqslant 0.35$ as can be seen from figure 1(a) which depicts the XRD profiles for $x = 0.35$. In the rhombohedral phase, the 200 pseudocubic peak is a singlet while the 222 pseudocubic peak is a doublet with the 222 reflection on the lower-2θ side of the $22\bar{2}$ reflection. The 220 set of reflections is also a doublet ($2\bar{2}0$ and 202) for the rhombohedral phase but the weaker 220 reflection occurs at the lower-angle side of the stronger $2\bar{2}0$ reflection, in marked contrast to that for the tetragonal phase. The structure of PMN–xPT for $x \leqslant 0.30$ is found to be rhombohedral as can be inferred from figure 1(c) which depicts the 200, 220 and 222 pseudocubic profiles for $x = 0.30$. Thus the MPB region, separating the tetragonal ($x \geqslant 0.35$) and rhombohedral ($x \leqslant 0.30$) phase fields, lies in the composition range $0.30 < x < 0.35$. The width of the MPB region in our samples is nearly an order of magnitude smaller than that reported by Kelly *et al* [17] and other workers [2, 18]. According to Kelly *et al* [17], the structure of the PMN–xPT is rhombohedral and tetragonal for $x \leqslant 0.26$ and $x \geqslant 0.65$ respectively. The narrow width of the MPB region in our samples is due

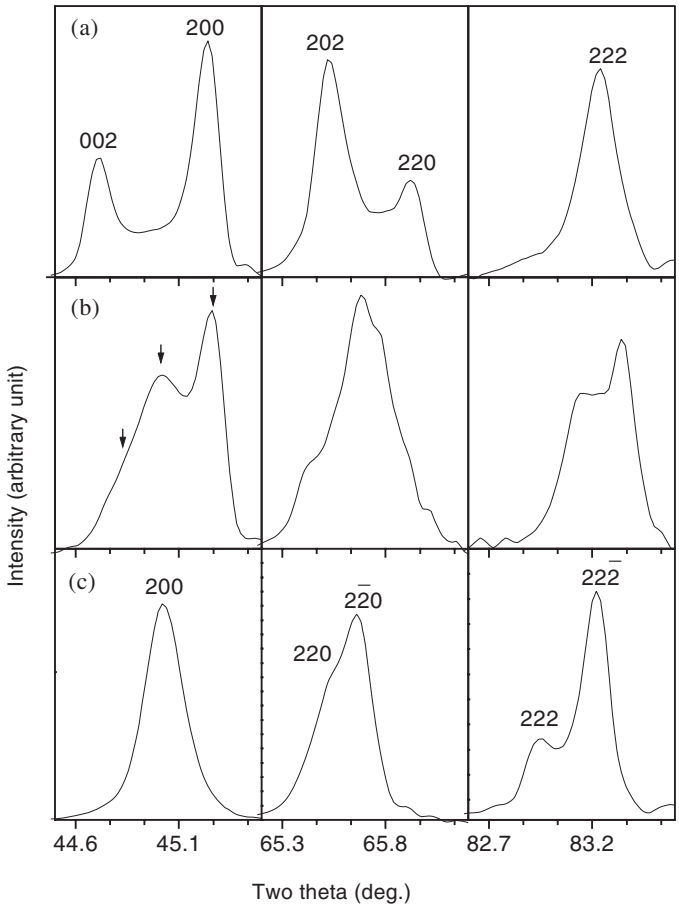

Figure 1. XRD profiles of 200, 220 and 222 pseudocubic reflections of $(1-x)[Pb(Mg_{1/3}Nb_{2/3})O_3]$–$xPbTiO_3$ at 300 K for (a) $x = 0.35$, (b) $x = 0.34$, (c) $x = 0.30$.

to the modifications introduced in the synthesis procedure which ensure excellent chemical homogeneity and perfect stoichiometry.

The 200 reflection of the rhombohedral phase occurs between the 002 and 200 peaks of the tetragonal phase. The presence of three peaks (marked with arrow) at the 200 pseudocubic position in figure 1(b) suggests that the structure of PMN–xPT with $x = 0.34$ (PMN–0.34PT) consists of a mixture of rhombohedral and tetragonal phases. In the PZT context, the structure of the MPB phase is found to be a mixture of tetragonal (space group $P4mm$) and monoclinic (space group Cm) [12], while in the PZN–xPT system it is reported to be pure monoclinic with space group Pm [14]. Yesu *et al* [14] have proposed that $Bmm2$ (or equivalently $Amm2$) is also a probable space group of the morphotropic phase in the PZN–xPT system. There are thus five different possibilities for the structure of the MPB phase in the PMN–xPT system: (i) a mixture of rhombohedral ($R3m$) and tetragonal ($P4mm$) phases; (ii) a pure monoclinic phase with space group Cm; (iii) a pure monoclinic phase with space group Pm; (iv) a mixture of tetragonal ($P4mm$) and monoclinic (Cm) phases; and (v) a pure orthorhombic ($Bmm2$) phase. In order to select the correct space group, Rietveld refinement was carried

Table 1. χ^2-values obtained after the Rietveld refinements for $0.66[Pb(Mg_{1/3}Nb_{2/3})O_3]$–$0.34PbTiO_3$ using different structural models.

Serial No	Structural model	χ^2
1	Mixture of rhombohedral ($R3m$) and tetragonal ($P4mm$)	4.05
2	Pure monoclinic phase (Cm)	4.10
3	Mixture of monoclinic (Cm) and tetragonal ($P4mm$)	3.65
4	Pure monoclinic phase (Pm)	3.43
5	Pure orthorhombic phase ($Bmm2$)	7.89

out using the DBWS-9411 program [19] for all five models mentioned above. In each of the refinements, a pseudo-Voigt function was used to define the peak profiles while a fifth-order polynomial was used for describing the background. Except for the occupancy parameters of the ions, which were kept fixed at the nominal composition, all other parameters, i.e., scale factor, zero correction, background, half-width parameters along with mixing parameters, lattice parameters, positional coordinates, and thermal parameters, were varied in the course of refinement. As in other Pb^{2+}-based perovskites, use of anisotropic thermal parameters for Pb^{2+} ions resulted in significant improvement in the R-factors for each model. We have also considered the off-centre displacement of the Pb^{2+} ion for producing local disorder as reported in case of tetragonal PZT [5, 20] but the R-factor was found to be much inferior. For other ions, only isotropic thermal parameters were refined. The refinement in all the cases converged smoothly after a few cycles.

In the tetragonal phase with $P4mm$ space group, the Pb^{2+} ion occupies 1(a) sites at $(0, 0, z)$, $Ti^{4+}/Nb^{5+}/Mg^{2+}$ and $O_{\rm I}^{2-}$ occupy 1(b) sites at $(1/2, 1/2, z)$ and $O_{\rm II}^{2-}$ occupy 2(c) sites at $(1/2, 0, z)$. For the rhombohedral phase with $R3m$ space group, we used hexagonal axes with lattice parameters $a_H = b_H = \sqrt{2}a_R$ and $c_H = \sqrt{3}a_R$ where a_R corresponds to the rhombohedral cell parameter. In the asymmetric unit of the structure of the rhombohedral phase with the $R3m$ space group, Pb^{2+} and $Nb^{5+}/Ti^{4+}/Mg^{2+}$ ions occupy 3(a) sites at $(0, 0, z)$ and O^{2-} ions occupy 9(b) sites at $(x, 2x, z)$. In the monoclinic phase with space group Cm, there are four ions in the asymmetric unit cell with Pb^{2+}, $Ti^{4+}/Nb^{5+}/Mg^{2+}$, and $O_{\rm I}^{2-}$ at 2(a) sites at $(x, 0, z)$ and $O_{\rm II}^{2-}$ at 4(b) sites at (x, y, z). The asymmetric unit cell of the monoclinic phase with space group Pm has five ions, with Pb^{2+} and $O_{\rm I}^{2-}$ at 1(a) sites at $(x, 0, z)$, $Ti^{4+}/Nb^{5+}/Mg^{2+}$, $O_{\rm II}^{2-}$, and $O_{\rm III}^{2-}$ at 1(b) sites at $(x, 1/2, z)$. Pb^{2+} was fixed at $(0, 0, 0)$ during refinement of the monoclinic structure. For the $Bmm2$ space group, Pb^{2+} ions occupy 2(b) sites at $(1/2, 1/2, z)$, $Nb^{5+}/Ti^{4+}/Mg^{2+}$ ions occupy 2(a) sites at $(0, 0, z)$, $O_{\rm I}^{2-}$ ions occupy 4(d) sites at $(x, 0, z)$, and $O_{\rm II}^{2-}$ ions occupy 2(b) sites at $(0, 1/2, z)$. $Nb^{5+}/Ti^{4+}/Mg^{2+}$ ions were kept at the origin $(0, 0, 0)$.

χ^2-values for PMN–0.34PT composition obtained after the refinements for the five different structural models are listed in table 1. It is evident from this table that the minimum value of χ^2 is obtained for the pure monoclinic phase model with space group Pm. It may be noted that the value of χ^2 for the model based on the coexistence of monoclinic (Cm) and tetragonal ($P4mm$) phases is not much higher than that for the Pm model. However, since the number of refinable structural parameters for the Pm model (20 parameters) is much smaller than that for the $Cm + P4mm$ model (28 parameters), Pm becomes the most plausible space group for the morphotropic phase of PMN–xPT. Thus the true symmetry of the MPB phase is monoclinic with space group Pm and not a mixture of rhombohedral and tetragonal phases as hitherto asserted in the PMN–xPT literature [17, 18].

Figure 2 depicts the observed, calculated, and difference profiles for the refined structure of the PMN–xPT powder with $x = 0.34$ for the monoclinic phase with space group Pm. The 'tick' marks above the difference profile in this figure give the positions of various reflections

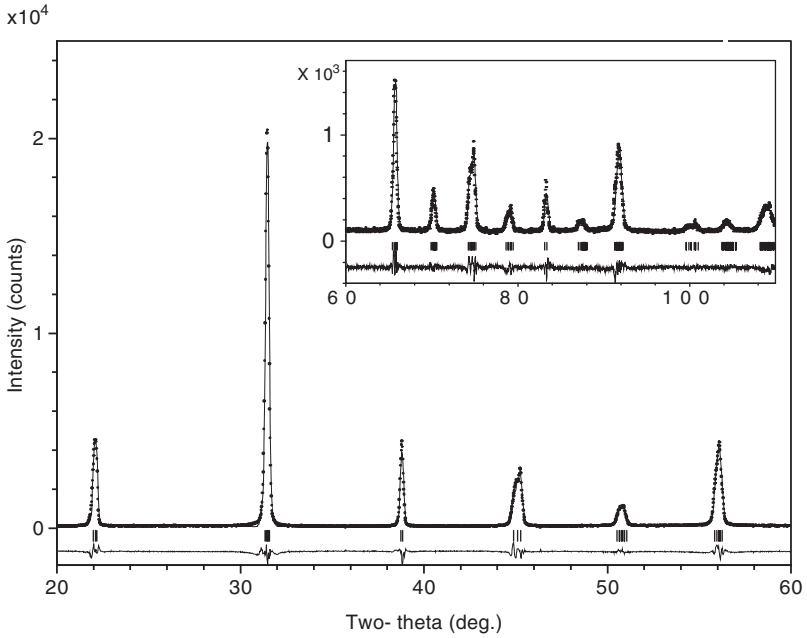

Figure 2. Observed (dots), calculated (continuous line), and difference (bottom line) profiles obtained from the Rietveld refinement of $(1-x)$[Pb($Mg_{1/3}Nb_{2/3}$)O_3]–xPbTiO_3 for $x = 0.34$ using the monoclinic space group Pm.

Table 2. Refined structural parameters of 0.66[Pb($Mg_{1/3}Nb_{2/3}$)O_3]–0.34PbTiO_3 for monoclinic structure with the space group Pm.

Monoclinic phase with space group Pm, $a = 4.0339(2)$ Å $b = 4.0016(2)$ Å, $c = 4.0157(2)$ Å, $\beta = 89.862(3)^\circ$				
Ions	x_M	Y_M	z_M	U (Å^2)
Pb^{2+}	0.00	0.00	0.00	$U_{11} = 0.059(1)$ $U_{22} = 0.054(2)$ $U_{33} = 0.050(2)$ $U_{13} = 0.027(2)$
$Ti^{4+}/Nb^{5+}/Mg^{2+}$	0.538(1)	0.50	0.538(2)	$U_{iso} = 0.089(2)$
O_I^{2-}	0.600(9)	0.00	0.50(1)	$U_{iso} = 0.11(1)$
O_{II}^{2-}	0.57(1)	0.50	0.02(1)	$U_{iso} = 0.51(2)$
O_{III}^{2-}	0.082(4)	0.50	0.555(8)	$U_{iso} = 0.47(2)$
R-factors	$R_{wp} = 11.83$	$R_{exp} = 6.36$	$R_B = 5.29$	$\chi^2 = 3.43$

for the Cu Kα_1 radiation. As is evident from this figure, the fit is quite good. Table 2 lists the refined structural parameters of the PMN–0.34PT. All the off-centre displacements of the ions responsible for the ferroelectric behaviour are in the (010) plane. The polarization vector can rotate in this plane only. The displacements of $Nb^{5+}/Ti^{4+}/Mg^{2+}$ in the [100] and [001] directions are found to be equal for PMN–0.34PT. This is possibly due to the close proximity of this composition ($x = 0.34$) to that for the onset of the tetragonal phase field ($x \geqslant 0.35$). As shown elsewhere [21], this equality of the displacement along [100] and [001] directions is not observed for other PMN–xPT compositions in the MPB region ($0.30 < x < 0.35$) with lower Ti^{4+} content.

The extension of Devonshire theory by Vanderbilt and Cohen [10] shows that the transition from the tetragonal to the monoclinic phase Pm (M_C-type in their notation) is of second-order type. This means that there cannot be coexistence of tetragonal ($P4mm$) and monoclinic (Pm) phases at the phase boundary. In fact, the refinement of the structure of PMN–0.34PT using a $P4mm+Pm$ model did not lead to any significant improvement in the R-factors commensurate with the increase in the number of refinable parameters (30 parameters) as compared to that for the pure Pm model (20 parameters). Thus our results clearly show that the tetragonal ($P4mm$) and monoclinic (Pm) regions are not separated by a two-phase region. The structure changes from monoclinic (Pm) to tetragonal ($P4mm$) very abruptly on increasing the Ti^{4+} content from $x = 0.34$–0.35. This abrupt change of structure also indicates a second-order nature of this phase boundary. The work of Vanderbilt and Cohen [10] predicts that the transition from the monoclinic (Pm) to the rhombohedral ($R3m$) phase should pass through an intermediate phase: either an orthorhombic ($Bmm2$) phase or another monoclinic phase of M_B (Cm space group) type. This possibility is currently being examined by us, but the preliminary results suggest the possibility of a monoclinic (M_B) phase between the monoclinic (Pm) and rhombohedral ($R3m$) regions.

To summarize, the structure of the morphotropic phase in the unpoled PMN–xPT system for $x = 0.34$ is monoclinic with space group Pm. This space group Pm is different from that (the Cm space group) of the monoclinic phase reported for the PZT system. It is, however, the same as that reported for the poled PZN–xPT system [22] for the morphotropic composition. The polarization vector in the monoclinic phase of the PMN–xPT system has components along [100] and [001] perovskite directions, in marked contrast to that in the monoclinic phase of PZT where the polarization components are along all three $\langle 100 \rangle$ perovskite directions.

References

[1] Jaffe B, Cook W R and Jaffe H 1971 *Piezoelectric Ceramics* (New York: Academic)
[2] Shrout T R, Jang J P, Kim N and Markgraf S 1990 *Ferroelectr. Lett.* **12** 63
[3] Kuwata J, Uchino K and Nomura S 1981 *Ferroelectrics* **37** 579
[4] Mishra S K, Singh A P and Pandey D 1997 *Phil. Mag.* B **76** 213
Mishra S K, Singh A P and Pandey D 1996 *Appl. Phys. Lett.* **69** 1707
Mishra S K and Pandey D 1997 *Phil. Mag.* B **76** 227
[5] Noheda B, Gonzalo J A, Guo R, Park S E, Cross L E, Cox D E and Shirane G 2000 *Phys. Rev.* B **61** 8687
[6] Noheda B, Cox D E, Shirane G, Guo R, Jones B and Cross L E 2000 *Phys. Rev.* B **63** 014103-1
[7] Guo R, Cross L E, Park S E, Noheda B, Cox D E and Shirane G 2000 *Phys. Rev. Lett.* **84** 5423
[8] Bellaiche L and Vanderbilt D 1999 *Phys. Rev. Lett.* **83** 1347
Bellaiche L, Gracia A and Vanderbilt D 2000 *Phys. Rev. Lett.* **84** 5427
[9] Ragini, Mishra S K, Pandey D, Lemmens H and Tendeloo G V 2001 *Phys. Rev.* B **64** 054101-1
[10] Vanderbilt D and Cohen M H 2001 *Phys. Rev.* B **63** 094108
[11] Ranjan R, Ragini, Mishra S K and Pandey D 2001 *Phys. Rev.* B at press
[12] Ragini, Ranjan R, Mishra S K and Pandey D 2001 *J. Appl. Phys.* submitted
[13] Ye Z G, Noheda B, Dong M, Cox D and Shirane G 2001 *Preprint* cond-mat/0107276
[14] Uesu Y, Matsuda M, Yamada Y, Fujishiro K, Cox D E, Noheda B and Shirane G 2001 *Preprint* cond-mat/0106552 v1
[15] Swartz S L and Shrout T R 1982 *Mater. Res. Bull.* **17** 1245
Bouquin O and Martine L 1991 *J. Am. Ceram. Soc.* **74** 1152
Wang H C and Schulze W A 1990 *J. Am. Ceram. Soc.* **73** 825
[16] Singh A K 2000 *MTech Materials Technology Thesis* Banaras Hindu University, India
[17] Kelly J, Leonard M, Tantigate C and Safari A 1997 *J. Am. Ceram. Soc.* **80** 957
[18] Noblanc O, Gaucher P and Calvarin G 1996 *J. Appl. Phys.* **79** 4291
[19] Young R A, Sakthivel A, Moss T S and Paiva Santos C O 1994 *Program DBWS-9411 for Rietveld Analysis of X-Ray and Neutron Powder Diffraction Patterns*
[20] Corker D L, Glazer A M, Whatmore R W, Stallard A and Fauth F 1998 *J. Phys.: Condens. Matter* **10** 6251
[21] Singh A K and Pandey D 2001 unpublished
[22] Noheda B, Cox D E, Shirane G, Park S E, Cross L E and Zhong Z 2001 *Phys. Rev. Lett.* **86** 3891